IOP Publishing Phys. Med. Biol. 69 (2024) 14TR01 https://doi.org/10.1088/1361-6560/ad539d

Physics in Medicine & Biology

IPEM Institute of Physics and Engineering in Medicine

OPEN ACCESS

RECEIVED
15 October 2023

REVISED
28 March 2024

ACCEPTED FOR PUBLICATION
3 June 2024

PUBLISHED
4 July 2024

TOPICAL REVIEW

Metrology for advanced radiotherapy using particle beams with ultra-high dose rates

Anna Subiel[1,2,*], Alexandra Bourgouin[3,10], Rafael Kranzer[4], Peter Peier[5], Franziska Frei[5], Faustino Gomez[6], Adrian Knyziak[7], Celeste Fleta[8], Claude Bailat[9] and Andreas Schüller[3]

[1] National Physical Laboratory, Hampton Road, Teddington TW11 0LW, United Kingdom
[2] University College London, Gower Street, London WC1E 6BT, United Kingdom
[3] Physikalisch-Technische Bundesanstalt (PTB), Braunschweig, Germany
[4] PTW-Freiburg, Lörracherstr. 7, 79115 Freiburg, Germany
[5] Federal Institute of Metrology METAS, Lindenweg 50, 3003 Bern-Wabern, Switzerland
[6] University of Santiago de Compostela, 15782 Santiago de Compostela, Spain
[7] Central Office of Measures (GUM), Elektoralna 2 Str., 00-139 Warsaw, Poland
[8] Instituto de Microelectrónica de Barcelona, Centro Nacional de Microelectrónica, IMB-CNM (CSIC), Barcelona, Spain
[9] Institute of Radiation Physics, Lausanne University Hospital and University of Lausanne, Lausanne, Switzerland
[10] National Research Council of Canada (NRC), 1200 Montreal Road, Ottawa, ON, K1A0R6, Canada
[*] Author to whom any correspondence should be addressed.

E-mail: anna.subiel@npl.co.uk

Keywords: dosimetry, calorimetry, Fricke, ionization chambers, flashDiamond, alanine, silicon carbide

Abstract

Dosimetry of ultra-high dose rate beams is one of the critical components which is required for safe implementation of FLASH radiotherapy (RT) into clinical practice. In the past years several national and international programmes have emerged with the aim to address some of the needs that are required for translation of this modality to clinics. These involve the establishment of dosimetry standards as well as the validation of protocols and dosimetry procedures. This review provides an overview of recent developments in the field of dosimetry for FLASH RT, with particular focus on primary and secondary standard instruments, and provides a brief outlook on the future work which is required to enable clinical implementation of FLASH RT.

Acronyms

BCT	beam current transformer
DPP	dose per pulse
GUM	Główny Urząd Miar
ICT	integrating current transformer
METAS	Federal Institute of Metrology METAS
NMI	National Metrology Institutes
NPL	National Physical Laboratory
PSPC	primary-standard proton calorimeter
PTB	Physikalisch-Technische Bundesanstalt
SiC	silicon carbide
SPGC	small portable graphite calorimeter
SSC	secondary standard calorimeter
UHDR	ultra-high dose rate
UHPDR	ultra-high pulse dose rate
UTIC	ultra-thin ionization chamber

1. Introduction

Radiotherapy (RT) used alone or in combination with other cancer treatment strategies has been proven to be the most cost-effective form of treatment (Barton *et al* 2014). Traditionally, RT has been delivered with a fractionation scheme, where typically 30 consecutive treatment sessions where a small amount of dose is

delivered over 5–6 weeks period to reduce the toxicity to the normal healthy tissues. This toxicity is the major limiting factor in curative outcomes of radiation treatment (Berkey 2010, Moding *et al* 2013) and is a catalyst for intense efforts to boost treatment efficacy by increasing the probability of tumour control and lowering the probability of normal tissue complication. In the recent years pre-clinical studies (Favaudon *et al* 2014, Loo *et al* 2017, Montay-Gruel *et al* 2017, 2018, 2019, Vozenin *et al* 2019) have demonstrated that treatment using ultra-high dose rates (UHDR) radiation exposures (averaged dose rate >40 Gy·s^{-1}) lead to remarkable sparing of healthy tissue whilst being at least as effective as treatments at conventional dose rates (∼2 Gy·min^{-1}) in controlling the tumour. This phenomenon has been named 'the FLASH effect' by the group which reignited interest in the UHDR irradiation in 2014 (Favaudon *et al* 2014). Since then, the research into this topic has steadily risen, with almost 600 papers related to FLASH and UHDR RT published up to date[11]. Majority of the published work has been conducted in the in preclinical settings (Schüler *et al* 2022). However, FLASH RT has already entered the phase of its clinical transfer with several veterinarian (Vozenin *et al* 2019, Konradsson *et al* 2021) and human clinical trials currently ongoing or concluded (Bourhis *et al* 2019, Daugherty *et al* 2022, 2023). Past shortfalls in physics and dosimetry reporting of preclinical and translational studies may have contributed to a reproducibility crisis of radiobiological data (Desrosiers *et al* 2013, Draeger *et al* 2020), but also highlighted the need for accurate and robust dosimetry. A dose verification survey of the pre-clinical irradiators has demonstrated that a number of facilities were not able to deliver the treatment within the 5% of the prescribed target dose and discrepancies between the aimed and the delivered dose were exceeding 40% (Pedersen *et al* 2016). Accurate dosimetry is crucial for the safe implementation of any RT technique, and it ensures best practice and consistency of treatments across radiation research centres and hospitals. To address this need, some international efforts have been initiated to provide FLASH community with adequate tools and dosimetry recommendations with the aim to support the translation of UHDR RT to clinical practice. The examples of such initiatives include (ii) AAPM TG-359 (2023) and (ii) the UHDpulse project (Schüller *et al* 2020). The latter one is the European project entitled 'Metrology for advanced RT using particle beams with ultra-high pulse dose rates' ((UHDpulse n.d.) (Schüller *et al* 2020)), which was established to provide a measurement framework, encompassing reference standards traceable to primary standards and validated reference methods for dose measurements at ultra-high pulse dose rates. The UHDpulse ended in February 2023, and this review outlines some of the significant outputs of that project and other developments in the field which support the translation of FLASH RT into clinics.

2. Primary standard methods for dosimetry of UHDR beams

All of the clinical RT treatments require provision of traceability chains to enable consistency of treatments across RT centres and modalities. All of those treatments need to be traceable to primary standards, which are made to the highest metrological quality and are maintained by the national metrology institutes. Up to now primary standards have not been established for the UHDR irradiations, hence so far the applicability of some of existing standards, in particular calorimeters and Fricke dosimeters, has been evaluated. Calorimeters have a number of advantages, which make them ideally suited for UHDR dosimetry. They can provide instant readout, are dose rate independent and allow for direct determination of the absorbed dose from fundamental principles. Calorimeters rely on measuring the radiation induced temperature rise in an absorber material as the initial energy of the impinging particle degrades to heat. Through knowledge of the material properties, including the specific heat capacity of the absorber, the rise in temperature can be converted to a measure of the absorbed dose. Moreover, thanks to ultra-short delivery times in UHDR exposures, uncertainties related to evaluation of heat transfer effects and determination of temperature rise itself will be smaller than in conventional dose rate RT. A recently published review by (Subiel and Romano 2023) provides a detailed overview of calorimeters and their application in UHDR dosimetry together with a list of advantages and disadvantages of calorimetric methods. In addition to calorimetry, Fricke dosimetry is an independent primary standard for absorbed dose to water in UHDR electron beams. It is a chemical dosimeter based on the oxidation of a closely water-equivalent ferrous ammonium sulphate solution when irradiated with ionizing radiation. Both methods, calorimetry and Fricke dosimetry, have been employed for absolute dosimetry in UHDR exposures and the output of the work is summarised in the following sections.

2.1. Fricke dosimetry for UHDR pulsed electron beams and absolute charge measurements

The standard Fricke solution (Fricke and Hart 1966) (1 mM Fe^{2+}, 0.4 M H_2SO_4, air saturated) is well established at conventional dose rate (∼1.5–2 Gy·min^{-1} at a repetition rate of 100 Hz) for absorbed dose to

[11] Pubmed search: ((((FLASH[Title]) AND (radiotherapy[Title])) OR (irradiations[Title])) OR (ultra-high dose rate[Title])) AND (irradiations[Title])

water in MeV pulsed electron beams (Pettersson and Hettinger 1967, Svensson and Brahme 1979, Rotblat *et al* 1997) (with the pulse duration of the order of few μs) and nearly independent on the dose rate up to ~2 Gy per pulse (Thomas and Hart 1962).

When Fricke solution is irradiated, Fe2+ ions oxidize to Fe3+. The resulting concentration of Fe3+ ions is usually determined by the change in absorbance of the solution at a wavelength of 304 nm using a UV spectrometer. This quantity is directly proportional to the absorbed energy. If the reaction of the Fricke solution to the total incident electron energy (radiation chemical yield), some independent physical quantities (such as the density and the optical path length in the solution during the absorbance measurement) and correction factors computed by Monte Carlo simulations (to account for the difference between water and Fricke solution and taking into account the influence of the holder) are known, the dose to water can be derived from this change in absorption (Vörös and Stucki 2007). In early experiments, Fricke dosimetry or ferrous sulphate dosimetry was often used as reference dose measurement in biological experiments with pulsed high dose rate electron beams (Town 1967, Zackrisson *et al* 1991). At Federal Institute of Metrology in Switzerland (METAS), sodium chloride (1 mM NaCl) is added to the Fricke solution to desensitize the system to organic impurities (Vörös *et al* 2012). However, this increases the dependence of the radiation chemical yield on the dose per pulse (DPP). For an electron pulse duration of 3 μs and the Fricke composition used at METAS, the correction was found to be smaller than 1% up to 0.4 Gy per pulse. As for the case without NaCl ICRU Report 34 (1982), this correction is nonlinear at higher DPP. For 10 Gy per pulse a correction of 10% was determined. On the other hand, increasing the iron concentration in the Fricke solution a reduction of the dose rate dependence is observed at the expense of the higher self-oxidation. This increases the susceptibility of the Fricke dosimeter to handling and impurities even further. The results obtained at METAS are in good qualitative agreement with those from previous work (Keene 1957, Schuler and Allen 1957, Sutton and Rotblat 1957, Fricke and Hart 1966, Sehested *et al* 1973, Rotblat *et al* 1997).

In order to make the Fricke dosimeter a primary standard, two steps are required.

First, a monoenergetic electron beam of known particle energy and beam charge is totally absorbed (Feist 1982) in a large volume of Fricke solution, allowing the determination of the response of the Fricke dosimeter (Vörös and Stucki 2007) as a function of the energy deposited by the beam. Amongst others, this requires an independent measurement of the absolute values of the beam charge. At METAS, an Integrating Current Transformer (ICT) (ICT-082-120-20:1) together with the corresponding electronics (CAC and BSP-IHR) from Bergoz Instrumentation (Saint Genis Pouilly, France) is used for this purpose. It was calibrated with a dedicated pulse generator provided by PTB. Based on previous work by Schüller *et al* (2017), PTB calibrated this pulse generator (built with components from CGC instruments) as a reference for calibration of devices for measurement of pulses of charge. For pulsed currents, special attention must be paid to the temporal structure of the charge in the pulse, any pre- and post-oscillations, and the rise and fall times. Devices that integrate in a specific time window are very sensitive to differences in the temporal current profile between the accelerator and the generator. To reach the desired uncertainty of the calibration, one must further account for the front-end, readout electronics and analysis.

As a second step, small bags ($30 \times 30 \times 3$ mm^3) filled with the same Fricke solution as described above, are irradiated in the reference UHDR electron beam. The absorbed dose is determined by using the previously derived response. Working standards, as for example ionization chambers (ICs) or alanine pellets, may be calibrated with this Fricke dosimeter (Vörös *et al* 2012).

2.2. Water calorimetry for UHDR pulsed electron beams

PTB worked on the development of a primary standard of absorbed dose to water in UHDR pulsed electron beams at the Metrological Electron Accelerator Facility (MELAF, Germany) (Schüller *et al* 2019). The existing PTB's primary standard water calorimeter (Krauss 2006), a sealed thin-walled plane-parallel glass vessel immersed in a water tank maintained at 4 °C, was validated in the UHDR reference electron beams at MELAF with a DPP ranging from 0.13 Gy to 6.3 Gy per pulse (2.5 μs pulse duration) (Bourgouin *et al* 2022c). The primary advantage of a water calorimeter is its direct measurement of dose in the relevant medium for medical physics, namely water. The PTB calorimeter (Krauss *et al* 2020) was used to disseminate the absolute dose to water for a range of total DPP (i) by modulating the instantaneous dose rate within a pulse of constant duration and (ii) by modifying the pulse duration with a constant instantaneous dose rate (Bourgouin *et al* 2023a). Heat transfer correction factors were determined via thermal simulations using the finite element method (FEM) in COMSOL Multiphysics v.5.6 (COMSOL AB, Stockholm, Sweden). Additionally, field perturbation and depth correction factors were assessed using the Monte Carlo method with the EGSnrc open-source software toolkit (Bourgouin *et al* 2023a). The results of the simulations have shown that the correction factors were comparable to the value found in the literature (Renaud *et al* 2020) despite the very short delivery time and the non-homogeneous (Gaussian) spatial dose distribution of the

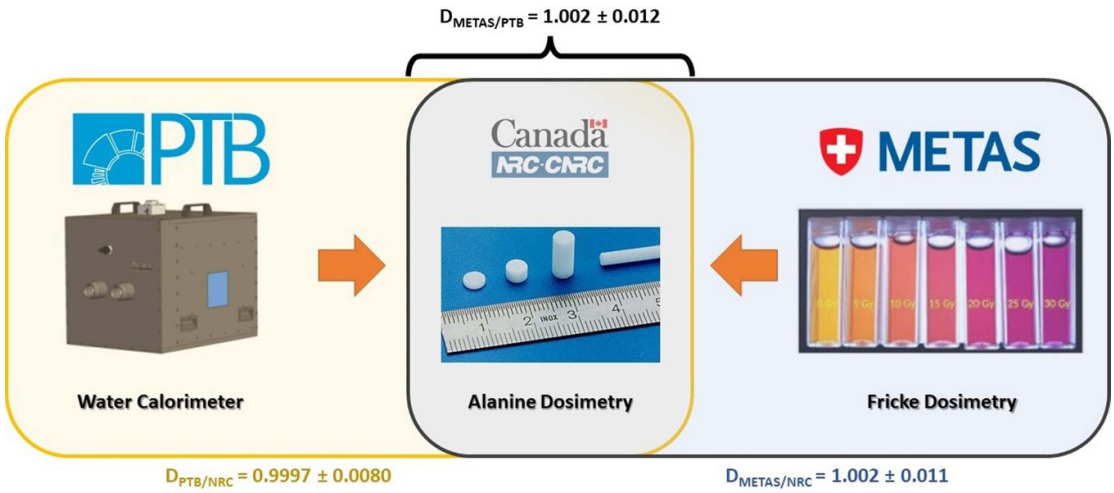

Figure 1. The intercomparison of PTB's and METAS' primary standard using NRC's alanine dosimetry system as a transfer standard.

reference UHDR pulsed electron beams. The largest impact of the very short total delivery time (few seconds), compared to the typical irradiation time required in conventional dose rate (>30 s up to 2 min), was on the analysis of the temperature-time trace used to determine the increase in temperature of the water. The temperature probe (a thermistor) of the calorimeter is embedded in glass which has a specific heat capacity about 5 times smaller than water. As a result, the temperature recorded by the probe is disturbed by the presence of the glass for about 40 s after the radiation ceased. Therefore, the temperature recorded within this time had to be discarded from the analysis. As reported in Bourgouin *et al* (2023a), the combined correction factors for the water calorimeter used in the reference UHDR electron beam was found to be within 0.99 and 1.01. The final combined standard uncertainty was evaluated to be less than 0.5%, which is the usual uncertainty target for a primary standard. The water calorimeter has been established as the primary standard for the UHDR reference electron beams at PTB.

2.3. Intercomparison of PTB and METAS primary standards in UHDR pulsed electron beam

One of the objectives of the UHDpulse project was to compare the respective primary standards of PTB and METAS in UHDR pulsed reference electron beam. For technical reasons, it was not possible to travel with any of the primary standards abroad. It was, therefore, decided to use alanine dosimeters as a transfer standard to carry out this comparison. Both institutes (i.e. PTB and METAS) irradiated alanine dosimeters, provided by the National Research Council of Canada (NRC), in their reference UHPDR electron beam and compared the result to a known absorbed-dose-to-water measurement traceable to their respective primary standards. By including the third institute in this comparison, i.e. the NRC, a clear separation was obtained between the primary standards involved in this comparison, as the used transfer standard (i.e. the alanine dosimeter) had an independent traceability route to the NRC's primary standard.

The ratio between the dose delivered by a calibrated UHPDR electron beam using the METAS primary standard, Fricke dosimeter, and the dose delivered by a calibrated UHPDR electron beam using the PTB primary standard, water calorimeter, was shown to be 1.002 ± 0.012, see figure 1. This work has demonstrated that both primary standards established in UHDR pulsed electron beam agree with each other within the combined standard uncertainty and showed suitability of alanine dosimeters as transfer detectors for such comparisons which offers a simpler route to wider-scale comparisons.

2.4. Graphite calorimetry for UHDR pulsed electron beams

The Polish National Metrology Institute, GUM, developed and characterized a portable graphite calorimeter as a primary standard for absorbed dose to water (Schüller *et al* 2020) for different conventional medical beams (photon, electrons and protons). It has a simplified typical calorimeter construction consisting of graphite elements (core, jacket, inner shield and outer shield) closed in a PMMA vacuum housing. Two sets including three thermistors, mounted in the core and jacket, are connected by two 30 m cables to the portable measuring system (3-channel Wheatstone direct current (DC) bridge, electrical calibrator). The portable graphite calorimeter was verified by a bilateral comparison with the NPL primary standard of absorbed dose to water for conventional photon beams. The difference between both standards was less than 0.5%. The GUM calorimeter was tested in PTB's ultra-high pulse dose rate reference electron beam within

the UHDpulse project (Bourgouin *et al* 2022c). The first step of the tests included the development of Monte Carlo models of the research accelerator and generation of the IAEAphsp files (defined as a collection of representative pseudo-particles emerging from a radiation therapy treatment source along with their properties that include energy, particle type, position, direction, progeny and statistical weight) using FLUKA for two different electron beam setups described by Bourgouin *et al* (2022c). The next step involved determination of correction factors based on IAEAphsp (Battistoni *et al* 2016), which included: the impurity correction factor (k_{imp}), and the gap correction accounting for the presence of non-graphite components and vacuum gaps within the calorimeter (k_{gap}), the water-to-graphite mass-stopping-power ratio ($s_{\mathrm{w,g}}$), and the fluence correction factor (k_{fl}), correcting for the difference in fluence at water-equivalent depths between water and graphite. The correction for radial non-uniformity in water was also applied. The depth-dose curve obtained from the Monte Carlo simulation was used for the determination of heat loss correction factor using FEM in FreeFem++ environment. The portable graphite calorimeter was operated in quasi-adiabatic mode with its core positioned at a reference depth in water of 5 g·cm^{-2}. The average absorbed dose to the core was determined by multiplying the measured increase in temperature by the specific heat capacity of the core, which was determined experimentally after each series of measurements during electric calibration. In following step, the value of the absorbed dose to water for 5 g·cm^{-2} was corrected for z_{ref}. at 4.65 g·cm^{-2}. The measurement frequency was 3 Hz or synchronized with the MELAF (Schüller *et al* 2019, Bourgouin *et al* 2022c). The calorimetric measurement procedure consisted of a series of six successive radiation exposures with a time gap of 120 s between each exposure. The expanded uncertainty of the measured dose is 0.57%. The results of measurements were compared with results of PTB alanine dosimeters. The results were within 0.2% agreement with combined uncertainty of 0.95% ($k = 2$).

2.5. Graphite calorimetry for UHDR proton beams

The NPL in support of implementation of the first in-human proton FLASH clinical trial at the Cincinnati Children's Hospital Medical Center (Lourenço *et al* 2023) performed measurements using the NPL PSPC (Lourenço *et al* 2022). Calorimetry measurements were carried out in six rectangular fields developed for the treatment of symptomatic bone metastasis, according to the requirements of the FAST-01 n.d clinical trial (Daugherty *et al* 2023), with an averaged dose rate of ∼63 Gy·s^{-1}, using a 250 MeV mono-energetic scanned layer. In this work, the calorimeter was operated in quasi-adiabatic mode with its core positioned at a reference depth in water of 5.2 g cm^{-2}. The average absorbed dose to the core was determined by multiplying the measured increase in temperature by the specific heat capacity of the core, which was determined experimentally at NPL (Williams *et al* 1993). The absorbed dose to water was determined as a product of absorbed dose to calorimeter core and the necessary beam-dependent correction factors which were determined using Monte Carlo simulations (Lourenço *et al* 2023). Those factors included k_{imp}, k_{gap}, $s_{\mathrm{w,g}}$ and k_{fl} (symbols explained in section 2.4). The numerical values of those factors have been published by Lourenço *et al* (2023). The overall uncertainty on the dose measured with the NPL's PSPC under proton FLASH conditions was 0.9% ($k = 1$) which was in line with recommendations for reference dosimetry in clinical RT (ICRU 1976, Karger *et al* 2010). Additionally, calorimetry measurements were compared against measurements performed with different types of ionisation chambers, to assess the feasibility of using these detectors in UHDR proton beams for reference dosimetry and quality assurance of treatments. PTW Farmer and Roos chambers exhibited significant ion recombination effects. However, the PTW Advanced Markus IC showed good agreement with the NPL PSPC and thus can be used for reference dosimetry as well as for quality assurance of FLASH proton pencil beam scanning treatments delivered by the isochronous cyclotrons at the averaged dose rate used in this work (up to 63 Gy s^{-1}) (Lee *et al* 2022). The ratios between the dose determined with the various ICs (Advanced Markus, Roos, PPC05 and Farmer) following TRS-398 Code of Practice (CoP) (TRS-398 2006) and the PSPC for different field sizes (from 5 × 6 cm^2 up to 5 × 12 cm^2) are shown in figure 2.

2.6. Simple calorimeters for dosimetry of UHDR beams

2.6.1. Secondary standard graphite calorimeter

A simple, low-cost secondary standard calorimeter (SSC) physically resembling a Roos-type IC has been realized by Bass *et al* (2023). The SSC incorporates only a single sensing thermistor in the 16 mm diameter, 2 mm thick aluminium core. The body of the calorimeter was 3D-printed from polylactic acid. This instrument has been used in a converted clinical electron LINAC to deliver UHDR 6 MeV electron beam (4 μs pulse duration) with an average dose rate of 180 Gy s^{-1} and 0.45 Gy pulse^{-1}. SSC was set up in a WTe[12] phantom at 70 cm source-to-surface distance with the reference point of the core at 13 mm water equivalent

[12] Water-equivalent material for clinically relevant electron beams produced by St Bartholomew's Hospital, London.

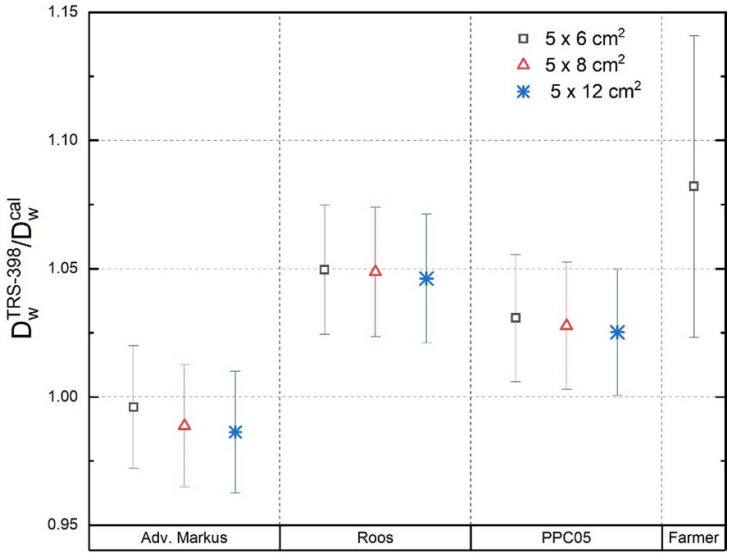

Figure 2. Ratios between the dose determined by the ionisation chambers (following TRS-398 protocol) and the NPL PSPC for the various fields tested. The error bars represent type A standard uncertainties (please note that uncertainty in determination of ion recombination is not included in the budget). The replotted data from the study of (Lourenço *et al* 2023).

depth, and 25 exposures of 400 pulses delivered. The calibration in terms of absorbed dose-to-water of the SSC has been performed against the NPL's primary standard electron graphite calorimeter (Bass *et al* 2023). The same corrections (see table 3 in Bass *et al* 2023) were applied to the primary standard calorimeter response in 6 MeV reference conditions to obtain dose in the UHDR mode. For more details see Bass *et al* (2023). The estimated standard uncertainty for this measurement was 1.25%.

2.6.2. Aluminium calorimeter

A simple open-to-atmosphere aluminium calorimeter was tested in the UHDR pulsed electron beam at the MELAF facility (Schüller *et al* 2019) at PTB to evaluate its applicability as a real-time dosimeter for UHDR pulsed electron beams (Bourgouin *et al* 2020). The design of the calorimeter was based on the NPL calorimeter for industrial processing dose measurement (Burns *et al* 1994). While a vacuum system is the most effective way to minimize heat loss for a solid-based calorimeter, it imposes significant limitations on the range of beams it can accommodate, as it necessitates sealing the calorimeter in a vacuum enclosure. In the context of FLASH RT research, characterized by significant variations in the characteristics of beams used, the flexibility derived from a simple open-to-atmosphere design proves to be a notable advantage. Moreover, as the dose is delivered within a few seconds or less, the imperative to reduce heat loss, compared to conventional dose rates, is substantially reduced. Very high-purity 99.999% aluminium had been chosen as an absorber for the calorimeter. The temperature of the 2.01 mm thick and 21.70 mm diameter aluminium core, was recorded through the change of resistance of a pair of thermistors. More details can be found in Bourgouin *et al* (2020). The calorimeter was exposed to a radiation field with a DPP ranging from 0.3 Gy to 1.8 Gy generated by a 50 MeV pencil electron beam broadened by the vacuum exit window made of copper and a 1 mm thick disk of aluminium and collimated with a 10 × 10 cm Elekta Precise standard clinical electron applicator.

The calorimeter dose response was shown to be linear within 0.5% with the beam pulse charge measured from an in-flange ICT. This simple open-to-atmosphere aluminium calorimeter was shown to be suitable for UHDR irradiations. However, further improvements are required to allow clinical implementation. This includes: (i) the determination of the dose conversion factor from the aluminium calorimeter core to water, (ii) improvements of the thermal insulation of the calorimeter to enhance its performance in the clinical environment and (iii) validation of the calorimeter as an absorbed dose standard.

2.6.3. SPGC calorimeter

The SPGC is a derivative of the previous instrument developed at NPL by McEwen and Duane (2000). Originally, the SPGC was intended for the measurement of low energy, clinical proton beams. However, more recently the device has been refurbished to be used under extreme conditions in a laser-driven proton beam. In such environment a significant electromagnetic pulse is generated through the laser-target interaction, and additional precautions described previously (Romano *et al* 2020, McCallum *et al* 2023) have been made

to enable calorimetric measurements. The SPGC is composed of a 20 mm diameter and 2 mm thickness cylindrical core containing 4 thermistors each coupled into separate arm of 4 DC Wheatstone bridge circuits. Small, expanded polystyrene beads, keep the core in place at the centre of a 22 mm diameter, 4 mm long air cavity. The core is enclosed by graphite jacket with 30 mm external diameter. The jacket is composed of three pieces: (i) lid, (ii) base and (iii) body arranged together, where the jacket lid has a thickness of 0.75 mm. A Styrofoam enclosure, designed to enhance thermal isolation, has been cut to size enabling exposure of the device in a confined space. SPCG was operated at the adiabatic mode. The measurements were conducted at the Central Laser Facility (CLF), Rutherford Appleton Laboratory (RAL) utilizing the high-power VULCAN-PW laser system. The laser at RAL was operated at full power with pulses of 600 J energy and approximately 500 fs duration directed onto (i) 15 μm gold and (ii) 1 μm polyethylene (CH plastic) targets. Additional energy dispersion of the accelerated proton beam has been introduced by 0.9 T dipole magnet. The SPGC was exposed to four (in total) shots generated using the laser system. The transversal dose profile inhomogeneity and the energy spectrum were variable on a shot-to-shot basis, also considering the different targets used, leading to a variation in the measurements of the delivered dose with the calorimeter (for more details see McCallum *et al* 2023). The values of the absorbed dose to the core retrieved in the calorimeter were variable from shot-to-shot. This was due to the fact that the deposited dose in the SPGC core was dependent on the stability of the laser energy, the pulse duration of the laser as well as the characteristics of the target from which the beam was accelerated. The mean dose to the graphite core ranging from 0.41 to 2.03 Gy has been recorded. The number of irradiations performed, limited the possibility to improve the statistical variability, verify the accuracy and access achievable uncertainties of this technique. However, the proof-of-principle of calorimetric measurements in laser-driven environment has been demonstrated.

3. Secondary standards and relative dosimetry for UHDR beams

ICs have been considered as the gold standard for reference dosimetry and are the most disseminated secondary standard for dosimetry since the start of RT (TRS-398 2006). Unfortunately, at ultra-high DPP, commercially available ICs suffer from significant saturation effects due to ion recombination (Petersson *et al* 2017, McManus *et al* 2020, Kranzer *et al* 2021, Paz-Martín *et al* 2022). The correction of such effects has been performed traditionally in the CoP with the two-voltage method (Almond *et al* 1999, TRS-398 2006) that can provide an accurate value for low DPP regime ($<$1 mGy per pulse) based on the Boag formalism (Boag 1950, Boag *et al* 1996). Such corrections are known to be inaccurate even for intra-operative RT modality (where DPP is up to 100 mGy) and another correction methods have been devised for such deliveries (Di Martino *et al* 2005, Laitano *et al* 2006). Specially in the electron FLASH beams, with instantaneous (intra pulse) dose rates up to several MGy s^{-1} (Felici *et al* 2020), the large density of drifting charge carriers within the active volume of the IC provokes a significant electric field perturbation, enhancing the ion recombination (Kranzer *et al* 2022b, Paz-Martín *et al* 2022). At the recommended operation voltage of 200 V, a Roos chamber can have charge collection efficiency (CCE) below 15% for a pulse of 6 Gy with a duration of 2.5 μs (Paz-Martín *et al* 2022). For the UHDR beam conditions plane parallel ICs are recommended over cylindrical ICs with similar electrode distance, due to the inhomogeneous electric field and the higher recombination fraction expected in the latter as a result. In the case of FLASH proton beams, the average dose rates are typically below 500 Gy s^{-1} (Darafsheh *et al* 2021, Leite *et al* 2023) with pulse repetition frequency between 750 to 1000 Hz for synchrocyclotrons (Darafsheh *et al* 2021) or in MHz range for isochronus cyclotrons (Leite *et al* 2023). Consequently, the beam could be considered as quasi-continuous and the dose rate is much lower than the instantaneous dose rate present in pulsed electron UHDR beams. Studies performed with Advanced Markus, CC01 and PPC05 ICs at 385 Gy s^{-1} show that charge readout for these chambers operated at 300 V exhibit saturation factors below 1.01 (Leite *et al* 2023, Lourenço *et al* 2023). These studies confirm that parallel plate chambers with electrode spacing below or equal to 1 mm have negligible correction from volume recombination and are suitable for proton absolute dosimetry in UHDR conditions. The experimental results for small gap chambers, like PPC05 (with electrode gap separation of 0.6 mm), when operated at high voltage (typically over 300 V) indicated the existence of some charge increase with higher applied voltage (Rossomme *et al* 2021). For this reason, the strategy of increasing the electric field in these chambers to reduce recombination, must be carried out carefully, trying to use a calibration coefficient and polarity effect correction factor evaluated at the voltage under consideration (TRS-398 2006).

Given a number of challenges in UHDR ionometry, detailed investigations aiming to improve the knowledge of ion recombination effect and other required corrections have been carried out within the scope of the UHDpulse project. The following sections summarize these investigations and discuss also other detectors such as alanine, flashDiamond, clinical calorimeter and SiC diodes which have been successfully used for relative dosimetry in UHDR conditions and have a potential to become secondary standard instruments for FLASH RT.

3.1. Ionization chambers (ICs)

The established ion recombination correction methods do not include the free electrons, which under UHDR pulsed beam delivery are the dominant component to the ion chamber signal. Although an effort has been recently performed by Fenwick and Kumar (2023) to improve the knowledge of the analytical parameterization of recombination considering the free electron contribution (Boag and Wilson 1952), this approach is still limited by the hypothesis of a constant chamber electric field. Alternatively, there are some phenomenological methods for the description of the recombination effect like the *logistic* formula (Petersson *et al* 2017), or some other analytical approximations (Di Martino *et al* 2005, Di Martino *et al* 2022a). A more elaborate approach, developed within the framework of the UHDpulse project, involves numerical simulation of electric field, charge drift, attachment and recombination describing the dynamical processes inside the sensitive volume of the IC (Gómez *et al* 2022, Kranzer *et al* 2022b, Paz-Martín *et al* 2022), based on the work of Gotz *et al* (2017). These models have shown an accurate description of IC CCE (see figure 3), also being capable to account for the time resolved current observed in the chamber (Paz-Martín *et al* 2022). However, the experimental determination of the CCEs of many ICs within UHDpulse (Bourgouin *et al* 2023b) indicates a considerable variation between chamber types with similar geometry and also between units of the same chamber model that can exceed 10% if CCE is low. Small differences in chamber geometry and construction may contribute significantly to the behaviour of commercially available chambers when CCE is below 90%. Additionally, it has been found that variations of air mass density can have also some impact on the CCE value. For example, a 4% discrepancy between METAS and PTB measurements for the same Advanced Markus chamber has been attributed to a 40 hPa pressure difference in agreement with numerical model simulations mentioned above (Bourgouin *et al* 2023b). For these reasons the use of any generic ion recombination correction factor for commercially available ICs under UHDR should be taken with considerable discretion.

Two different strategies have been taken to build parallel plate ICs that can work under UHDR conditions with CCE close to 100%. In the first approach, in the study carried out by Di Martino *et al* (2022b), a gas with higher electron mobility (i.e. noble gas) operated at low pressure has been used in order to have a fast negative charge carrier collection and negligible ion recombination that was expected from the theoretical study of the authors, to work up to 40 Gy per pulse with a CCE higher than 99%. In the second approach, the role of the distance between electrodes of vented ICs has been studied experimentally (Cavallone *et al* 2022, Kranzer *et al* 2022b, Liu *et al* 2024) where in the work of Kranzer *et al* (2022b) the measurements with parallel plate chambers with same design but manufactured with 1 mm, 0.5 mm and 0.25 mm electrode distance are also well described with numerical simulations. The experimental results show that this parameter is the most relevant to achieve operation with small recombination losses under UHDR conditions. Furthermore, for two chambers with voltages U_1 and U_2 and electrode separations d_1 and d_2, compatible charge collection efficiencies were found whenever $U_1/{d_1}^2 = U_2/{d_2}^2$. In this way the same recombination loss is expected for a chamber with double electrode distance when the operating voltage is quadruple. The use of a very small electrode distance of 0.25 mm in air vented ICs (Gómez *et al* 2022, Kranzer *et al* 2022b), the so called UTIC with several prototypes built and already tested, leads to an effective free electron fraction over 98% for a bias voltage of 300 V with CCE higher than 99% for a 2.5 μs pulse of 5 Gy. One of the issues of the construction of ultra-thin chambers is the fact that small deviations of the geometrical dimensions can have significant effects on the chamber performance. Figure 3 represents the behaviour of the UTIC (red open circles) and the CCE when operated in the pulsed UHDR electron beam. For comparison two different commercially available parallel plate ICs (PTW Advanced Markus T34045 and Roos T34001) are also included in figure 3.

Both chamber designs, ALLS and UTIC, approach the physical limits of ionization mode operation, since they have to deal with an appropriate chamber configuration to avoid charge multiplication due to electron collisions in the active volume, either due to the large electron mean free path at low pressure (for ALLS) or due to the high electric field value at atmospheric conditions (for UTIC) (Gómez *et al* 2022, Kranzer *et al* 2022b). In the case of the UTIC the relative effect of charge multiplication is around 2% for a bias voltage of 500 V. Experimental results indicate that for chambers with small electrode distance in UHDR electron beams, CCE can also depend on pulse duration, not only on the DPP (Paz-Martín *et al* 2022). At the current stage of development of the understanding of ion chamber operation under UHDR conditions, it is advisable to perform the dosimetry studies not only reporting the DPP but also the pulse duration and pulse repetition rate. In summary, the UTICs, developed within the UHDpulse project, are excellent candidates for secondary standards for dosimetry in UHDR beams considering that they are waterproof, easy to handle and can be directly applied following the existing methodology in current CoPs.

3.2. Alanine dosimetry

Alanine is an amino acid that once irradiated gives rise to the generation of free radicals which are directly proportional to the total absorbed dose. The radicals are detected through electron spin resonance (EPR)

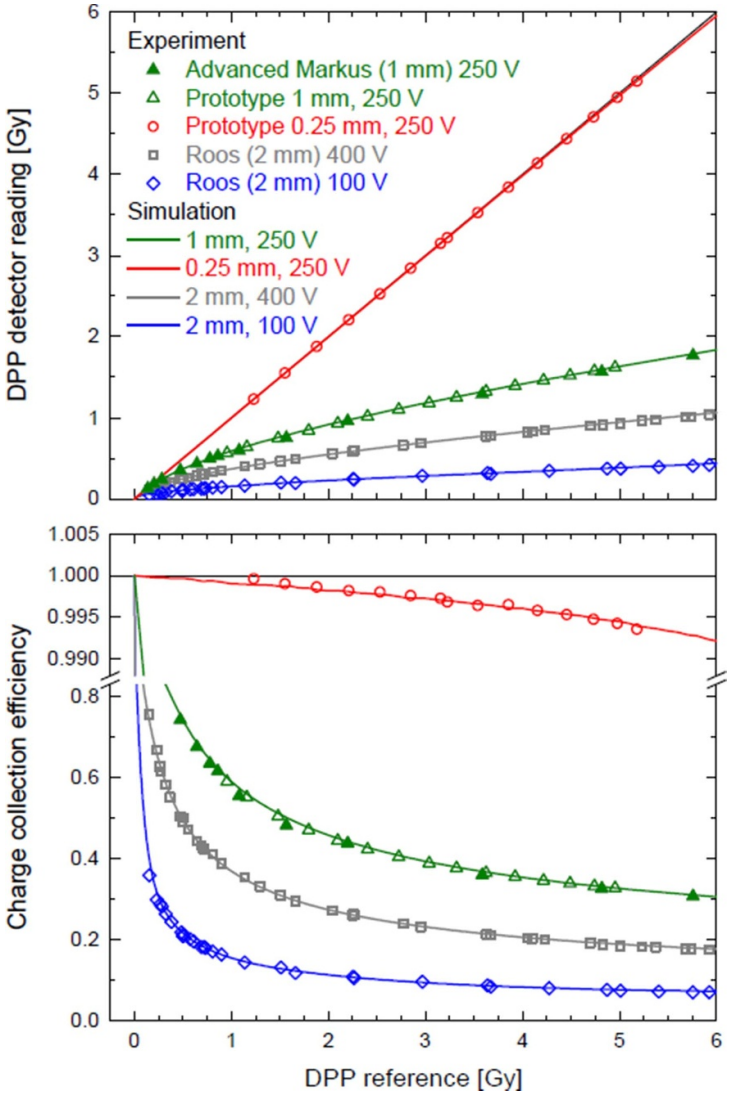

Figure 3. Upper panel: detector reading of the dose per pulse in a water phantom at reference depth from different parallel plate ionization chambers (Advanced Markus, Roos and two prototypes with 1 mm and 0.25 mm electrode gap separation) without correction for ion recombination effects as function of the actual dose per pulse from experiment (symbols) and simulations (lines) for different electrode distances and operational voltages. The prototypes share the same design but have different electrode distance, 1 mm (like Advanced Markus) and 0.25 mm (UTIC). Lower panel: charge collection efficiency from the same data as shown in the upper panel. Note the different scaling after the axis break. For details see Kranzer *et al* (2022b) and Paz-Martín *et al* (2022).

spectroscopy. The dose to water is then obtained from a series of correction and conversion factors and a calibration in a reference ^{60}Co beam (Anton 2006, Vörös *et al* 2012, Anton *et al* 2013, McEwen *et al* 2020). Alanine dosimeters are frequently employed for industrial applications (Sharpe *et al* 1996) where high doses are delivered at a high dose rate. They are suitable for UHDR beams since no dose-response dependency has been observed even for extremely high dose rates (Kudoh *et al* 1997). Alanine dosimeter responds linearly for dose deposited between 2 Gy to 5 kGy (Nagy *et al* 2002) and no significant dose-rate dependency was observed as a function of dose delivered up to 5 kGy (Desrosiers *et al* 2008). The lack of dose rate dependence has been also confirmed in a UHDR electron beams with a clinical uncertainty level, i.e. $<1\%$ ($k = 1$) at PTB (Bourgouin *et al* 2022a) it has been validated directly against primary standard water calorimeter (Bourgouin *et al* 2022a).

Alanine dosimeters are commonly used in commissioning, characterization, and calibration of UHDR electron beams at the PTB (Bourgouin *et al* 2022a), research centres (Stephan *et al* 2022), and hospitals (Jorge *et al* 2022). They are also used for investigating the responses of other passive detectors, including optically stimulated luminescence detectors, thermally stimulated luminescence detectors (Motta *et al* 2023), and Gafchromic films. Moreover, alanine dosimeters have been used as reference dosimeters in numerous studies involving commercially available ion chambers (Petersson *et al* 2017, Soliman *et al* 2020, Kranzer *et al* 2021, Bourgouin *et al* 2022b) and models under development (Kranzer *et al* 2021, Gómez *et al* 2022). They also

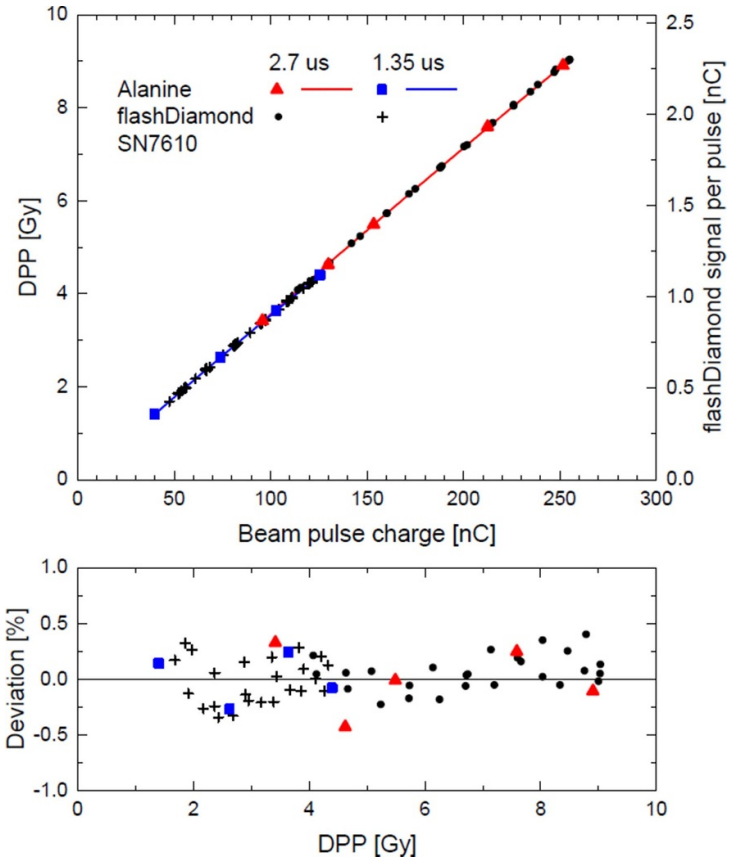

Figure 4. Upper panel: dose per pulse in a water phantom measured by means of PTB's alanine dosimetry system as function of the charge per pulse measured by means of an integrating current transformer for 2.7 μs (red triangles) and 1.35 μs (blue squares) beam pulse duration. Lines: interpolation functions. Dots and crosses represent results from measurements by means of a flashDiamond prototype (SN7610) at the same position as the alanine pellets shortly before as well as after the alanine irradiation. Right axis indicates the corresponding signal from the flashDiamond in terms of emitted charge per pulse. Lower panel: relative deviation from interpolation line in the upper panel as a function of DPP as measured by alanine or the flashDiamond, respectively.

serve as valuable tools in the development and validation of solid-state detectors, e.g. SiC (Romano *et al* 2023) and diamond detectors (Kranzer *et al* 2022a). The upper panel of figure 4 presents the DPP measured with PTB's alanine dosimetry system as a function of the beam pulse charge measured by an ICT at PTB together with the DDP measured by a flashDiamond detector (discussed in section 3.3). The two dosimeters agree well with the uncertainties. Since the dose is proportional to the number of primary electrons, there is a linear relationship between DPP and beam pulse charge. The lower panel of figure 4 presents the relative deviations of the measured DPP values from the interpolation line in the upper panel, revealing a precision below 0.5%.

Biological studies on the FLASH effect also employed alanine detectors for validation of dosimetry. In 2019, Jorge *et al* published dosimetric and preparation procedures for irradiating biological models to study the FLASH effect using passive detectors including alanine (Jorge *et al* 2019). *In vivo* dose measurement was performed using alanine pellets in FLASH effect studies on cats, mini-pigs (Vozenin *et al* 2019), and mice (Singers Sørensen *et al* 2022). Alanine dosimeters were also used in the first human treatment employing FLASH RT (Bourhis *et al* 2019).

The biggest challenge in establishing alanine dosimetry as a secondary standard for UHDR beams in research is the required expertise, specialized equipment, and the time necessary to achieve high accuracy and low uncertainty of measurement. The precision and accuracy of the determination of absorbed dose to water relies mostly on the evaluation of the mass and EPR signal of the alanine pellet, but also an accurate calibration. The calibration process to achieve high accuracy, with standard combined uncertainty $<1\%$, is time-consuming. Most commercial EPR dosimetry systems are not designed for measuring alanine pellets' signal exposed to low doses such as 10 Gy, which are typical dose levels for therapeutic applications, and accurate dose calibration is very challenging. Many publications reporting preclinical results of the FLASH effect supported by passive dosimetry have been employing alanine. The optimization process to achieve the highest signal-to-noise ratio while minimizing the readout time, to deliver results promptly for UHDR beams in pre-clinical experiments has been reported by Gondré *et al* (2020). Following a systematic

optimization, alanine dosimetry can reach an accuracy of around 2% ($k = 1$) for dose levels between 10 and 100 Gy in a pre-clinical setting. However, alanine dosimetry used as a secondary standard can reach an uncertainty below 1% ($k = 1$) when performed at a National Metrology Institute (Bourgouin *et al* 2022a). As the implementation of an alanine/EPR system in the clinic can be quite challenging, it is therefore recommended to take advantage of a mail alanine dosimetry service such as the ones provided by NPL (Sharpe and Sephton 1988) or NRC (Mansour 2018).

3.3. Flash diamond

As described in the UHDpulse introductory paper by Schüller *et al* (2020), the commercially available diamond detector, the PTW microDiamond 2024 (mD) (Bagalà *et al* 2013, Di Venanzio *et al* 2013, Laub and Crilly 2014, Pimpinella *et al* 2015), is suitable for clinical electron beam dosimetry in conventional RT and intraoperative radiation therapy and offers good radiation hardness. The properties of the mD under UHDR conditions were investigated using various samples and modified designs by Marinelli *et al* (2022) and Kranzer *et al* (2022a). These studies have shown that, in general, the mD is not suitable for dosimetry of UHDR pulsed electron beams. Even if there are some samples that show a linearity of up to 2 Gy per pulse and thus reach the UHDPP range, most saturate at around 200 mGy per pulse (Kranzer *et al* 2022a, Di Martino *et al* 2023). The manufacturer's specification for the maximum DPP is 100 mGy (microDiamond 2024). The crucial properties to improve the DPP response linearity of the detector are the sensitivity and the total series resistance, which can be adjusted by the doping concentration in the p-type layer of the diamond's Schottky-diode. The optimization of these parameters led to development of a novel detector called the flashDiamond (fD). This new detector was thoroughly tested in pulsed electron beams (table 1) and showed very good linearity of its response as a function of the DPP. In Marinelli *et al* (2022), linearity was achieved up to a DPP of 25 Gy with a pulse duration of 4 μs. Figure 5 shows the superior performance of the fD (blue and red symbols) with respect to commercially available mDs. The deviation from linearity of commercially available fDs type 60 025 is less than 3% up to 2 Gy μs^{-1} according to the vendors specification (microDiamond 2024). But there are although samples which show no significant deviation up to at least 4 Gy μs^{-1}. Such a fD, cross-calibrated against alanine measurements (see figure 4), is currently used at PTB as complementary reference. Furthermore, the fD shows an excellent temporal resolution. With a suitable readout chain, it is possible to measure the individual pulses of an electron accelerator with high time resolution and thus to determine not only the DPP but also the shape and duration of the pulse. By using a transimpedance amplifier and a digital oscilloscope, a temporal resolution in the range of a few ns could be achieved (Marinelli *et al* 2023). Additionally, the temporal structure of scanned pencil beams can also be detected (Tessonnier *et al* 2023).

Moreover, fD demonstrated excellent performance for relative dose distribution, i.e. percentage depth dose (PDD) curves and lateral dose profiles, as well as the output factor measurements (Verona Rinati *et al* 2022, Di Martino *et al* 2023). The usability and properties of the fD were validated in four different UHDR pulsed electron accelerators, three of which are commercially available for research in FLASH RT. During the investigations at PTB's ultra-high pulse dose rate reference electron beam (Bourgouin *et al* 2022c), no significant influence of the accumulated dose on the dose-response of the detector has been observed. This was checked by repeatedly comparing the linearity and response against the current transfer integrated and calibrated as a monitor system in the beamline. During the ongoing tests, a dose of up to 3 MGy was accumulated. The results of these investigations demonstrated that the fD can successfully perform relative three-dimensional dose distribution measurements in both conventional and UHDR modes without the need to apply dose conversion and correction factors, unlike for commercially available air-filled ICs operated in the UHDR beams (Petersson *et al* 2017).

The fD has also the potential to be used as a secondary standard instrument for the determination of the absolute absorbed dose to water in UHDR beams. However, the methodology for the determination of the absolute dose and for the establishment of a traceability chain is still under investigation. In the meanwhile, a cross-calibration against a suitable reference, such as a calibrated ionisation chamber in conventional RT beam, could be a viable option for research applications.

3.4. Graphite probe calorimeter

The graphite probe calorimeter, known as Aerrow, has been developed at McGill University by Renaud *et al* (2018) for dosimetry in the clinical environment. The calorimeter is designed as a nested cylindrical arrangement of graphite components with dimensions similar to a Farmer ion chamber with a buildup cap. The sensitive volume, made of a 6.1 mm diameter by 10.0 mm long graphite core, is separated from a 0.7 mm thick jacket by a 0.7 mm layer of rigid silica aerogel insulation. An additional 1.0 mm layer of aerogel thermally isolates the jacket from a 1.0 mm thick graphite shield. As the calorimeter was designed for a clinical environment, the solid insulation provides mechanical support, maintaining a constant relative

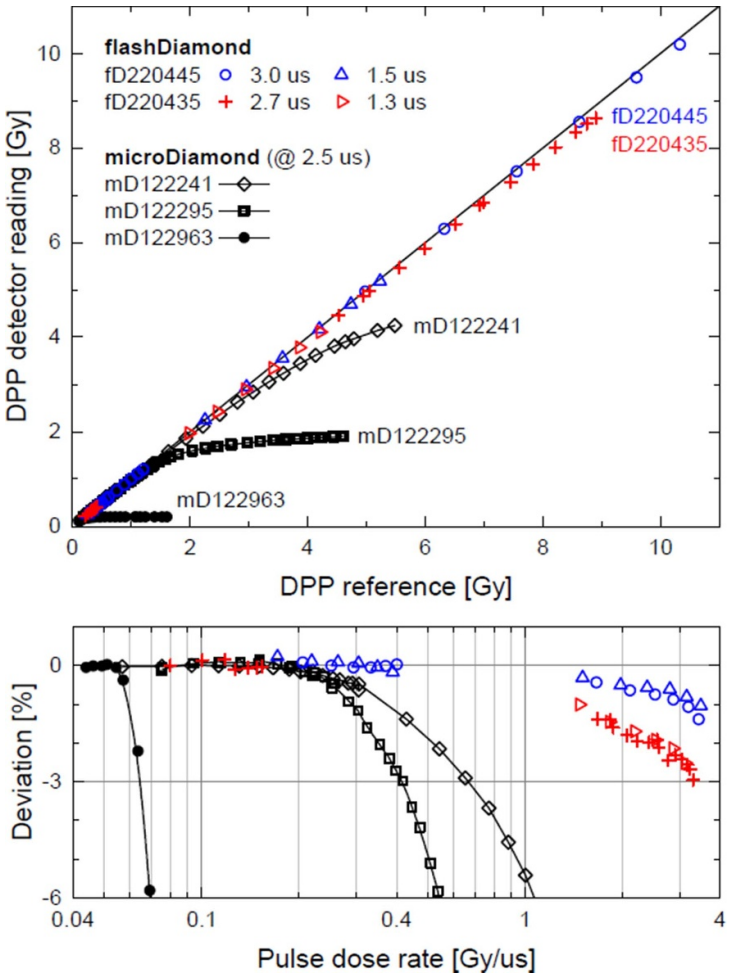

Figure 5. Upper panel: detector reading of the measured dose per pulse as function of the actual dose per pulse in a water phantom for three commercially available microDiamond detectors (PTW T60019) under the same beam conditions (2.5 us pulse duration) as well as for two commercially available flashDiamond detectors (PTW T60025) at different pulse durations. Lower panel: relative deviation of detector reading as function of the pulse dose rate.

positioning of the graphite components for user-friendly handling. It can be easily transported between research centres and requires no more user handling than an ion chamber.

To evaluate the suitability of the probe calorimeter as a relative and absolute secondary standard for UHDR pulsed electron beam (Bourgouin *et al* 2022c), the calorimeter was tested at the UHDR reference electron beam facility at PTB (Bourgouin *et al* 2022b). In this investigation, the calorimeter was exposed to a range of DPP up to 5.6 Gy. The influence on the calorimeter's response with the number of pulses delivered per measurement was also evaluated along with a depth dose curve measurement to evaluate the potential of the calorimeter for relative dosimetry. The absolute dose deposited per pulse was compared to the dose obtained with a calibrated Advanced Markus ionisation chamber, corrected for the ion recombination effects by means of alanine dose measurements.

Aerrow was shown to be suitable for relative and absolute dosimetry in the UHDR pulsed electron beam. The depth dose curve measured with Aerrow was in good agreement with the Monte Carlo calculated PDD profile (Bourgouin *et al* 2022b). The absolute dose to water determined with Aerrow was consistent, within stated uncertainty at $k = 1$, with the calibrated Advanced Markus ionisation chamber. The investigation also demonstrated the independence of the calorimeter's dose-response on the number of pulses delivered. The total combined standard uncertainty for the absolute dose measurement was evaluated to be 1.06% (Bourgouin *et al* 2022b). The Aerrow probe calorimeter is a real-time detector which could offer fully automated data acquisition and analysis, providing a great advantage over passive dosimetry systems such as alanine dosimetry. Also, the uncertainty could be further reduced to achieve the target uncertainty for clinical applications, $<1\%$, by measuring precisely the thermal properties of the insulation material found in the graphite probe, the aerogel. Currently, its' heat conductivity is not precisely known, which is greatly affecting the uncertainty of the heat transfer correction factor which is the largest component of the combined relative standard uncertainty.

3.5. SiC diodes

SiC is a wide band-gap semiconductor with unique properties that make it an interesting alternative for radiation detection applications in extreme conditions (Sellin and Vaitkus 2006, Nava *et al* 2008). SiC has a large displacement energy threshold (30–40 eV) which makes it intrinsically radiation hard. Its ionisation energy of 7.8 eV is a factor of two higher than for silicon, resulting in a lower sensitivity per unit volume and deposited dose. This makes it a better choice for dosimetry in UHDR beams, where the large signal might saturate the semiconductor. Compared to diamond, SiC is cheaper and has a more mature technology allowing to produce larger and more complex structures.

The first characterization of SiC diodes with UHDR pulsed beams was reported in 2023 by Romano *et al* (2023). They measured the response of a 1×1 cm^2 SiC diode with 9 MeV electrons accelerated by a dedicated ElectronFLASH LINAC. The SiC diode showed a linear response up to at least 1.77 Gy per pulse (with 2 μs pulse duration, 30 Hz repetition rate) when using a diode bias voltage of 480 V. Both the diode leakage current and the charge signal were stable up to at least 90 kGy of accumulated dose, proving the good radiation hardness of the SiC material to electron beams. In a more recent publication, the same group have reported similar results with the produced SiC detectors up to 5 Gy per pulse at 4 μs pulse duration (Milluzzo *et al* 2023).

In the framework of the UHDPulse project, the Institute of Microelectronics of Barcelona (IMB-CNM, CSIC) produced SiC diodes specifically designed for UHDR dosimetry (Fleta 2024). The circular diodes had 1 mm diameter and a multi-guard ring configuration and were manufactured in epitaxial 4H-SiC wafers. They were encapsulated by PTW Freiburg with the microSilicon package (Schönfeld *et al* 2019) to provide electrical connectivity and waterproofing, and were characterized in PTB's UHDR reference electron beam (Bourgouin *et al* 2022c). The SiC diode was operated without external bias voltage. The diode response was independent both of DPP and of instantaneous dose rate for 20 MeV electrons up to 11 Gy per pulse and 3.8 Gy μs^{-1}, respectively, with a relative deviation below 3%. For comparison, commercial silicon diode dosimeters tested under similar conditions start to show a saturated response at hundreds of mGy per pulse for electrons (dose rates tens of Gy s^{-1}) (Di Martino *et al* 2020, Konradsson *et al* 2020). The long-term sensitivity reduction (i.e. after several kGy) of the SiC diode with 20 MeV electrons accumulated dose was 0.018% kGy^{-1}. In a relative dosimetry measurement, the acquisition of a PDD profile in UHDR conditions, the SiC diode performed comparably well to a reference flashDiamond (Fleta 2024). This work demonstrated for the first time the suitability of SiC diodes for relative dosimetry in UHDR pulsed electron beams up to a DPP of 11 Gy.

3.6. Beam current transformers (BCTs)

Conventional monitoring systems are semi-transparent ICs. They cannot be used as monitoring systems in UHDR mode, due to their optimization for conventional dose rates. BCTs are used in many particle accelerators for diagnostics and monitoring (Unser 1981, 1985, Bergoz 1991, Schütte and Unser 1992, Unser 1992, Torp *et al* 1994). BCTs are robust and non-destructive, and they measure the induced current of passing through charged particles. In addition, they also provide information on the beam's temporal structure. PTB uses a BCT from Bergoz Instrumentation (ICT) for determination of the charge per beam pulse (Schüller *et al* 2017) at their ultra-high pulse dose rate reference electron beam (see figure 4). High precision BCTs from Bergoz Instrumentation using a toroid sensor, an external electronic system and a power supply were tested on two UHDR accelerators, namely on the Oriatron eRT6 linac (PMB ALCEN, France) and the Mobetron (IntraOp, Sunnyvale, CA, USA). Two BCTs were located at the exit of the linacs, operating at 10 mA (peak current) and 300 mA (peak current) when using UHDR beam parameters (Oesterle *et al* 2021, Gonçalves Jorge *et al* 2022). More recently, Liu *et al* (2023) successfully tested dual BCT configuration in the FLASH Mobetron system for beam control and monitoring for electron FLASH RT. BCT have shown adequate dose and dose rate linearity as well as beam parameter recording for beam monitoring of pulsed electron beam delivered in conventional and UHDR. The absorbed dose can be derived and measured in real-time during irradiations. The delivered dose can be estimated with an accuracy required for pre-clinical studies using specific calibration factors for each geometry. In effect, the beam transport between the BCT and the target can modify the BCT calibration factor drastically due to scattering effects or applicator collimation. Therefore, it is recommended to obtain calibration factors using reference dosimeters placed at the target location in the real geometry.

4. Conclusions and future outlook

This review presents a comprehensive overview of primary and secondary standard instruments which have been tested under UHDR conditions (table 1). Due to UHDRs and pulsed structure of the beams used in the FLASH RT studies, direct application of dosimetry protocols designed for conventional RT is currently impossible without additional considerations. It is essential that national metrology institutes provide

Table 1. The summary of devices and their applications in UHDR beams.

Device/instrument	UHDR beam modality	Energy (MeV)	DPP (Gy)	Instantaneous dose rate (Gy μs^{-1})	Average dose rate (Gy s^{-1})	Pulse duration (μs)	Pulse repetition rate (Hz)	Standard uncertainty	Availability	References
					Primary standards					
Fricke dosimetry (METAS)	Electrons	15	0.1–10	0.033–3.3	1–10	3	10	0.93%	NMI:METAS	—
PTB's water calorimeter	Electrons	20	0.1–10	0.04–4.0	1–50	1.2–2.8	5	0.49%	NMI:PTB	(Bourgouin *et al* 2023a)
GUM's graphite calorimeter	Electrons	20	0.1–10	0.04–4.0	1–10	2.5	5	0.57%	NMI:GUM	—
NPL's PSPC	Protons	250	N/A	6.3 × 10^−5	63		Quasi continuous	0.90%	NMI:NPL	(Lee *et al* 2022) (Lourenço *et al* 2022)
					Portable simple calorimeters					
SSC	Electrons	6	∼0.45	∼0.11	180	4	200	1.25%	NPL	(Bass *et al* 2023)
Aluminium calorimeter	Electrons	50	0.2–1.8	0.1–0.7	1.5–9	2.5	5	—	NRC	(Bourgouin *et al* 2020)
SPGC	Laser-accelerated protons	15–40	1–3	1000	N/A	0.001	Single pulse	—	NPL	(Romano *et al* 2020) (McCallum *et al* 2023)

(Continued.)

Table 1. (Continued.)

Potential secondary/tertiary standards										
UTIC	Electrons	9 20	1–10 1.2–5.4	0.25–2.5 0.48–2.2	10–100 6–27	4 2.5	10 5	1.40%	Under development	(Kranzer *et al* 2021) (Gómez *et al* 2022) figure 3
Alanine	Electrons	20	0.15–9	0.15–3.3	0.75–45	1.35, 2.5, 2.7	5	0.85%	Commercial (through calibration laboratories)	(Bourgouin *et al* 2023a) Figure 4
flashDiamond	Electrons	7, 9 20	0.3–26 0.2–10	0.5–6.6 0.15–3.3	Up to 960 1–50	1–4 1.35–3	5−245 5	1% @ 0.25 Gy μs^{-1} 3% @ 2.5 Gy μs^{-1}	Commercial	(Kranzer *et al* 2022a) (Marinelli *et al* 2022) (Marinelli *et al* 2023) (Tessonnier *et al* 2023) (Verona Rinati *et al* 2022) (Di Martino *et al* 2023) figure 5
SiC diode	Electrons	20 9	0.4–11 0.02–5	0.7–3.8 0.01–1.2	2–55 0.6–53	2.9, 1.6, 0.5 2, 4	5 30	3% —	Under development	(Fleta 2024) (Romano *et al* 2023) (Milluzzo *et al* 2023)
Aerrow graphite probe calorimeter	Electrons	20	0.6–5.6	0.24–2.24	3–28	2.5	5	1.06%	Commercial	(Bourgouin *et al* 2023b)
Commercially available ionization chambers	Electrons Protons (PBS)	20 227	0.14–6.2 4.3, 17.5, and 38.1	0.352–2.48 4 × 10^−6– 3.85 × 10^−3	0.7–31 4–385	2.5 1 × 10^6, 99 × 10^3	5 Single pulse (PBS)	2.5% up to 10% [a] 1.5%[b]	Commercial	(Bourgouin *et al* 2023b) (Leite *et al* 2023)

(Continued.)

Table 1. (Continued.)

Device/instrument	UHDR beam modality	Energy (MeV)	DPP (Gy)	Instantaneous dose rate (Gy μs^{-1})	Average dose rate (Gy s^{-1})	Pulse duration (μs)	Pulse repetition rate (Hz)	Standard uncertainty	Availability	References
					Beam monitors					
BCT	Electrons	4–10	0.005–100	0.0017–35	0.05–100	1	10	1.00%	Commercial	(Gondré *et al* 2020) (Oesterle *et al* 2021) (Gonçalves Jorge *et al* 2022) (Liu *et al* 2023)

[a] The uncertainty estimated depends on the method used to evaluate the effect due to ion recombination.

[b] Ion recombination correction factors below 2% were obtained for most chambers.

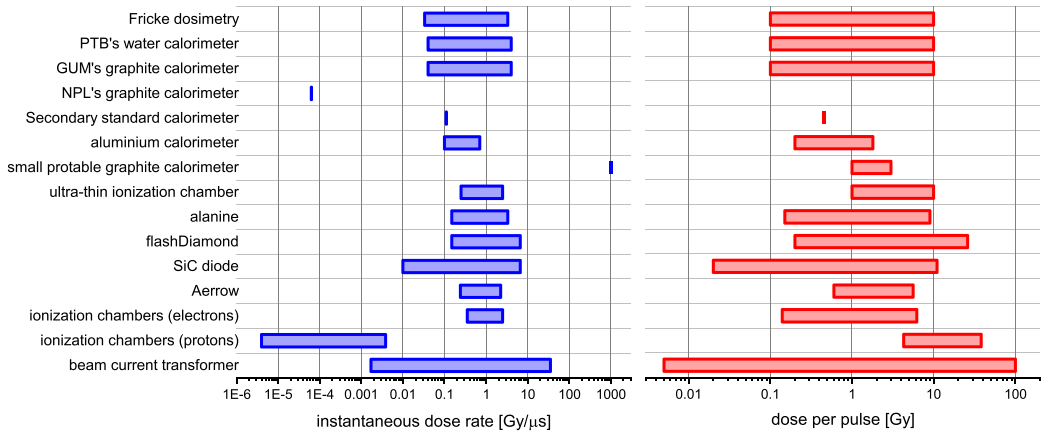

Figure 6. A wide range of instantaneous dose rates and dose per pulse used for dosimetric studies presented in this review.

adequate traceability routes for FLASH RT for both, clinical and pre-clinical, applications. This involves establishment of primary standards for UHDR beams, which are able to realize the absorbed-dose-to-water with a standard uncertainty equivalent to conventional dose-rate RT (i.e. below 0.5%). The accuracy of these standards is demonstrated by their degrees of equivalence resulting from several international comparisons (Picard *et al* 2015, 2017). So far only three national metrology institutes: PTB, METAS and NPL evaluated their primary standard instruments for application in UHDR electron and proton beams operated under certain beam parameters (see table 1 for details). However, more work is required to provide evidence of equivalency of different primary standards used under UHDR exposures by carrying out international comparisons. This should be done under International Bureau of Weights and Measures (BIPM)[13] umbrella (The BIPM key comparison database 2023). After adaptation and establishment of primary standards for UHDR beams, it is essential to secure traceability of secondary standard instruments for reference dosimetry. Several detectors have been successfully tested under UHDR conditions, including simple calorimeters (section 2.6), new designs of ICs (section 3.1), flashDiamond (section 3.3) and SiC detectors (section 3.5). These detectors demonstrated desirable characteristics when operated under UHDR conditions, which make them promising candidates as secondary standard devices for FLASH RT. However, significant amount of work needs to be carried out to perform full characterization and establish long-term stability of these devices. Moreover, it is not clear which machine beam parameters: DPP, instantaneous dose rate or perhaps an average dose rate are the most critical for determination/optimization of FLASH effect. Figure 6 demonstrates a wide range of instantaneous dose rates and DPP used in various dosimetry studies presented in this review. It is still unclear whether current dosimetry protocols, after adaptation for UHDR conditions, could be used, but it is hoped that in the next years working groups such as AAPM TG-359 (2023) will be able to provide dosimetry guidelines for the FLASH community. This review outlines current state-of-the-art of dosimetry in FLASH RT. However, this rapidly developing field is constantly growing. Therefore, in the next years we should see further advances in the field, which will play very important role in enabling translation of FLASH RT to clinical practice.

Acknowledgments

We would like to acknowledge Malcolm McEwen, James Renaud and Bryan Muir who made contributions to content of this work. Furthermore, we would like to thank Marco Marinelli and Gianluca Verona Rinati for their valuable contribution to the development of the flashDiamond, produced at the Faculty of Industrial Engineering of the University of Rome-Tor Vergata.

Funding

This project 18HLT04 UHDpulse has received funding from the EMPIR programme co-financed by the Participating States and from the European Union's Horizon 2020 research and innovation programme.

[13] The BIPM is the coordinator of the world-wide measurement system, ensuring it gives comparable and internationally accepted measurement results.

Conflict of interest

Rafael Kranzer is employee of PTW Freiburg. The remaining authors declare that the research was conducted in the absence of any commercial or financial relationships that could be construed as a potential conflict of interest.

ORCID iDs

Anna Subiel https://orcid.org/0000-0002-3467-4631
Alexandra Bourgouin https://orcid.org/0000-0001-6429-4122
Rafael Kranzer https://orcid.org/0000-0003-4063-0413
Celeste Fleta https://orcid.org/0000-0002-6591-6744
Andreas Schüller https://orcid.org/0000-0002-0355-299X

References

Almond P R, Biggs P J, Coursey B M, Hanson W F, Huq M S, Nath R and Rogers D W 1999 AAPM's TG-51 protocol for clinical reference dosimetry of high-energy photon and electron beams *Med. Phys.* **26** 1847–70
Anton M 2006 Uncertainties in alanine/ESR dosimetry at the Physikalisch-Technische Bundesanstalt *Phys. Med. Biol.* **51** 5419–40
Anton M, Kapsch R P, Krauss A, von Voigts-rhetz P, Zink K and McEwen M 2013 Difference in the relative response of the alanine dosimeter to megavoltage x-ray and electron beams *Phys. Med. Biol.* **58** 3259–82
Bagalà P *et al* 2013 Radiotherapy electron beams collimated by small tubular applicators: characterization by silicon and diamond diodes *Phys. Med. Biol.* **58** 8121–33
Barton M B, Jacob S, Shafiq J, Wong K, Thompson S R, Hanna T P and Delaney G P 2014 Estimating the demand for radiotherapy from the evidence: a review of changes from 2003 to 2012 *Radiother. Oncol.* **112** 140–4
Bass G A, Shipley D R, Flynn S F and Thomas R A S 2023 A prototype low-cost secondary standard calorimeter for reference dosimetry with ultra-high pulse dose rates *Br. J. Radiol.* **96** 20220638
Battistoni G *et al* 2016 The FLUKA code: an accurate simulation tool for particle therapy *Front. Oncol.* **6** 116
Bergoz J 1991 Current monitors for particle beams *Nucl. Phys.* A **525** 595–600
Berkey F J 2010 Managing the adverse effects of radiation therapy *Am. Fam. Phys.* **82** 381–8, 394 (available at: www.aafp.org/pubs/afp/issues/2010/0815/p381.html)
Boag J W 1950 Ionization measurements at very high intensities. Pulsed radiation beams *Br. J. Radiol.* **23** 601–11
Boag J W, Hochhäuser E and Balk O A 1996 The effect of free-electron collection on the recombination correction to ionization measurements of pulsed radiation *Phys. Med. Biol.* **41** 885–97
Boag J W and Wilson T 1952 The saturation curve at high ionization intensity *Br. J. Appl. Phys.* **3** 222
Bourgouin A, Hackel T and Kapsch R P 2023a The PTB water calorimeter for determining the absolute absorbed dose to water in ultra-high pulse dose rate electron beams *Phys. Med. Biol.* **68** 115016
Bourgouin A, Hackel T, Marinelli M, Kranzer R, Schüller A and Kapsch R P 2022a Absorbed-dose-to-water measurement using alanine in ultra-high-pulse-dose-rate electron beams *Phys. Med. Biol.* **67** 205011
Bourgouin A, Keszti F, Schönfeld A A, Hackel T, Kozelka J, Hildreth J, Simon W, Schüller A, Kapsch R P and Renaud J 2022b The probe-format graphite calorimeter, Aerrow, for absolute dosimetry in ultrahigh pulse dose rate electron beams *Med. Phys.* **49** 6635–45
Bourgouin A, Knyziak A, Marinelli M, Kranzer R, Schüller A and Kapsch R-P 2022c Characterization of the PTB ultra-high pulse dose rate reference electron beam *Phys. Med. Biol.* **67** 085013
Bourgouin A, Paz-Martín J, Can Gedik Y, Frei F, Peier P, Rossomme S, Schönfeld A, Schüller A, Gomez Rodriguez F and Kapsch R-P 2023b Charge collection efficiency of commercially available parallel-plate ionisation chambers in ultra-high dose-per-pulse electron beams *Phys. Med. Biol.* **68** 235002
Bourgouin A, Schüller A, Hackel T, Kranzer R, Poppinga D, Kapsch R-P and McEwen M 2020 Calorimeter for real-time dosimetry of pulsed ultra-high dose rate electron beams *Front. Phys.* **8** 567340
Bourhis J *et al* 2019 Treatment of a first patient with FLASH-radiotherapy *Radiother. Oncol.* **139** 18–22
Burns D T, McEwen M R and Williams A J 1994 *An NPL Absorbed Dose Calibration Service for Electron Beam Radiotherapy* (International Atomic Energy Agency (IAEA))
Cavallone M, Gonçalves Jorge P, Moeckli R, Bailat C, Flacco A, Prezado Y and Delorme R 2022 Determination of the ion collection efficiency of the razor nano chamber for ultra-high dose-rate electron beams *Med. Phys.* **49** 4731–42
ClinicalTrials.gov Identifier: NCT04986696 2023 (https://clinicaltrials.gov/ct2/show/NCT04986696)(Accessed 03 August 2023)
Darafsheh A, Hao Y, Zhao X, Zwart T, Wagner M, Evans T, Reynoso F and Zhao T Y 2021 Spread-out Bragg peak proton FLASH irradiation using a clinical synchrocyclotron: proof of concept and ion chamber characterization *Med. Phys* **48** 4472–84
Daugherty E C *et al* 2022 FAST-01: results of the first-in-human study of proton FLASH radiotherapy *Int. J. Radiat. Oncol. Biol. Phys.* **114** S4
Daugherty E C *et al* 2023 FLASH radiotherapy for the treatment of symptomatic bone metastases (FAST-01): protocol for the first prospective feasibility study *JMIR Res. Protocols* **12** e41812
Desrosiers M F, Puhl J M and Cooper S L 2008 An absorbed-dose/dose-rate dependence for the alanine-EPR dosimetry system and its implications in high-dose ionizing radiation metrology *J. Res. Natl Inst. Stand. Technol.* **113** 79–95
Desrosiers M, DeWerd L, Deye J, Lindsay P, Murphy M K, Mitch M, Macchiarini F, Stojadinovic S and Stone H 2013 The importance of dosimetry standardization in radiobiology *J. Res. Nat. Inst. Stand. Technol.* **118** 403
Di Martino F *et al* 2020 FLASH radiotherapy with electrons: issues related to the production, monitoring, and dosimetric characterization of the beam *Front. Phys.* **8** 570697
Di Martino F *et al* 2022a A new calculation method for the free electron fraction of an ionization chamber in the ultra-high-dose-per-pulse regimen *Phys. Med.* **103** 175–80

Di Martino F et al 2022b A new solution for UHDP and UHDR (Flash) measurements: theory and conceptual design of ALLS chamber *Phys. Med.* **102** 9–18
Di Martino F et al 2023 Architecture, flexibility and performance of a special electron linac dedicated to Flash radiotherapy research: electronFlash with a triode gun of the Centro Pisano flash radiotherapy (CPFR) *Front. Phys.* **11** 1268310
Di Martino F, Giannelli M, Traino A C and Lazzeri M 2005 Ion recombination correction for very high dose-per-pulse high-energy electron beams *Med. Phys.* **32** 2204–10
Di Venanzio C, Marinelli M, Milani E, Prestopino G, Verona C, Verona-Rinati G, Falco M D, Bagalà P, Santoni R and Pimpinella M 2013 Characterization of a synthetic single crystal diamond Schottky diode for radiotherapy electron beam dosimetry *Med. Phys.* **40** 021712
Draeger E, Sawant A, Johnstone C, Koger B, Becker S, Vujaskovic Z, Jackson I L and Poirier Y 2020 A dose of reality: how 20 years of incomplete physics and dosimetry reporting in radiobiology studies may have contributed to the reproducibility crisis *Int. J. Radiat. Oncol. Biol. Phys.* **106** 243–52
Favaudon V et al 2014 Ultrahigh dose-rate FLASH irradiation increases the differential response between normal and tumor tissue in mice *Sci. Transl. Med.* **6** 245ra293
Feist H 1982 Determination of the absorbed dose to water for high-energy photons and electrons by total absorption of electrons in ferrous sulphate solution *Phys. Med. Biol.* **27** 1435
Felici G et al 2020 Transforming an IORT linac into a FLASH research machine: procedure and dosimetric characterization *Front. Phys.* **8** 374
Fenwick J D and Kumar S 2023 Collection efficiencies of ionization chambers in pulsed radiation beams: an exact solution of an ion recombination model including free electron effects *Phys. Med. Biol.* **68** 015016
FLASH radiotherapy for the treatment of symptomatic bone metastases in the thorax (FAST-02) (available at: https://clinicaltrials.gov/ct2/show/NCT05524064)
Fleta C, Pellegrini G, Godignon P, Gómez Rodríguez F, Paz-Martín J, Kranzer R and Schüller A 2024 State-of-the-art silicon carbide diode dosimeters for ultra-high dose-per-pulse radiation at FLASH radiotherapy *Phys. Med. Biol.* **69** 095013
Fricke H and Hart E 1966 Chemical dosimetry *Radiation Dosimetry* (Academic)
Gómez F et al 2022 Development of an ultra-thin parallel plate ionization chamber for dosimetry in FLASH radiotherapy *Med. Phys.* **49** 4705–14
Gonçalves Jorge P, Grilj V, Bourhis J, Vozenin M C, Germond J F, Bochud F, Bailat C and Moeckli R 2022 Technical note: validation of an ultrahigh dose rate pulsed electron beam monitoring system using a current transformer for FLASH preclinical studies *Med. Phys.* **49** 1831–8
Gondré M, Jorge P G, Vozenin M C, Bourhis J, Bochud F, Bailat C and Moeckli R 2020 Optimization of alanine measurements for fast and accurate dosimetry in FLASH radiation therapy *Radiat. Res.* **194** 573–9
Gotz M, Karsch L and Pawelke J 2017 A new model for volume recombination in plane-parallel chambers in pulsed fields of high dose-per-pulse *Phys. Med. Biol.* **62** 8634–54
Bass G A, Manning J W, Homer M J, Shipley D R and Barry M A 2023 The NPL absorbed dose to water primary standard for electron beams: summary of factors incorporating ICRU Report 90 recommendations 2023 *NPL Report. IR 64*
ICRU Report 24 1976 Determination of absorbed dose in a patient irradiated by beams of x or gamma rays in radiotherapy procedures (The International Comission on Radiation Units) (available at: www.scirp.org/reference/referencespapers?referenceid=1637422)
ICRU Report 34 1982 *The Dosimetry of Pulsed Radiation* (The International Comission on Radiation Units)
Jorge P G et al 2019 Dosimetric and preparation procedures for irradiating biological models with pulsed electron beam at ultra-high dose-rate *Radiother. Oncol.* **139** 34–39
Jorge P G et al 2022 Design and validation of a dosimetric comparison scheme tailored for ultra-high dose-rate electron beams to support multicenter FLASH preclinical studies *Radiother. Oncol.* **175** 203–9
Karger C P, Jäkel O, Palmans H and Kanai T 2010 Dosimetry for ion beam radiotherapy *Phys. Med. Biol.* **55** R193–234
Keene J P 1957 The oxidation of ferrous ammonium sulfate solutions by electron irradiation at high dose rates *Radiat. Res.* **6** 424–9
Konradsson E, Arendt M L, Bastholm Jensen K, Børresen B, Hansen A E, Bäck S, Kristensen A T, Munck Af Rosenschöld P, Ceberg C and Petersson K 2021 Establishment and initial experience of clinical FLASH radiotherapy in canine cancer patients *Front. Oncol.* **11** 658004
Konradsson E, Ceberg C, Lempart M, Blad B, Bäck S, Knöös T and Petersson K 2020 Correction for ion recombination in a built-in monitor chamber of a clinical linear accelerator at ultra-high dose rates *Radiat. Res.* **194** 580–6
Kranzer R, Poppinga D, Weidner J, Schüller A, Hackel T, Looe H K and Poppe B 2021 Ion collection efficiency of ionization chambers in ultra-high dose-per-pulse electron beams *Med. Phys.* **48** 819–30
Kranzer R, Schüller A, Bourgouin A, Hackel T, Poppinga D, Lapp M, Looe H K and Poppe B 2022a Response of diamond detectors in ultra-high dose-per-pulse electron beams for dosimetry at FLASH radiotherapy *Phys. Med. Biol.* **67** 075002
Kranzer R, Schüller A, Gómez Rodríguez F, Weidner J, Paz-Martín J, Looe H K and Poppe B 2022b Charge collection efficiency, underlying recombination mechanisms, and the role of electrode distance of vented ionization chambers under ultra-high dose-per-pulse conditions *Phys. Med.* **104** 10–17
Krauss A 2006 The PTB water calorimeter for the absolute determination of absorbed dose to water in 60Co radiation *Metrologia* **43** 259
Krauss A, Renkamp C K and Klüter S 2020 Direct determination of k B →,Q,Q0 for cylindrical ionization chambers in a 6 MV 0.35 T MR-linac *Phys. Med. Biol.* **65** 235049
Kudoh H, Celina M, Kaye R J, Gillen K T and Clough R L 1997 Response of alanine dosimeters at very high dose rate *Appl. Radiat. Isot.* **48** 497–9
Laitano R F, Guerra A S, Pimpinella M, Caporali C and Petrucci A 2006 Charge collection efficiency in ionization chambers exposed to electron beams with high dose per pulse *Phys. Med. Biol.* **51** 6419–36
Laub W U and Crilly R 2014 Clinical radiation therapy measurements with a new commercial synthetic single crystal diamond detector *J. Appl. Clin. Med. Phys.* **15** 4890
Lee E et al 2022 Ultrahigh dose rate pencil beam scanning proton dosimetry using ion chambers and a calorimeter in support of first in-human FLASH clinical trial *Med. Phys.* **49** 6171–82
Leite A M M, Cavallone M, Ronga M G, Trompier F, Ristic Y, Patriarca A and De Marzi L 2023 Ion recombination correction factors and detector comparison in a very-high dose rate proton scanning beam *Phys. Med.* **106** 102518
Liu K, Holmes S, Hooten B, Schüler E and Beddar S 2024 Evaluation of ion chamber response for applications in electron FLASH radiotherapy *Med. Phys.* **51** 494–508

Liu K, Palmiero A, Chopra N, Velasquez B, Li Z, Beddar S and Schüler E 2023 Dual beam-current transformer design for monitoring and reporting of electron ultra-high dose rate (FLASH) beam parameters *J. Appl. Clin. Med. Phys.* **24** e13891
Loo B, Schuler E, Lartey F, Rafat M, King G, Trovati S, Koong A and Maxim P 2017 (P003) Delivery of ultra-rapid flash radiation therapy and demonstration of normal tissue sparing after abdominal irradiation of mice *Int. J. Radiat. Oncol. Biol. Phys.* **98** E16
Lourenço A *et al* 2023 Absolute dosimetry for FLASH proton pencil beam scanning radiotherapy *Sci. Rep.* **13** 2054
Lourenço A, Lee N, Shipley D, Romano F, Kacperek A, Duane S, Cashmore M, Bass G, Palmans H and Thomas R 2022 Application of a portable primary standard level graphite calorimeter for absolute dosimetry in a clinical low-energy passively scattered proton beam *Phys. Med. Biol.* **67** 225021
Mansour I 2018 Development of mailed dosimetric audit for external beam radiation therapy using alanine dosimeters *MSc Thesis* Carleton University
Marinelli M *et al* 2022 Design, realization, and characterization of a novel diamond detector prototype for FLASH radiotherapy dosimetry *Med. Phys* **49** 1902–10
Marinelli M, Di Martino F, Del Sarto D, Pensavalle J H, Felici G, Giunti L, De Liso V, Kranzer R, Verona C and Verona Rinati G 2023 A diamond detector based dosimetric system for instantaneous dose rate measurements in FLASH electron beams *Phys. Med. Biol.* **68** 175011
McCallum S, Lee N, Milluzzo G, McIlvenny A, Borghesi M, Subiel A and Romano F 2023 Proof-of-principle of absolute dosimetry using an absorbed dose portable calorimeter with laser-driven proton beams *Appl. Sci.* **13** 11894
McEwen M R and Duane S 2000 A portable calorimeter for measuring absorbed dose in the radiotherapy clinic *Phys. Med. Biol.* **45** 3675–91
McEwen M, Miller A, Pazos I and Sharpe P 2020 Determination of a consensus scaling factor to convert a Co-60-based alanine dose reading to yield the dose delivered in a high energy electron beam *Radiat. Phys. Chem.* **171** 108673
McManus M, Romano F, Lee N D, Farabolini W, Gilardi A, Royle G, Palmans H and Subiel A 2020 The challenge of ionisation chamber dosimetry in ultra-short pulsed high dose-rate very high energy electron beams *Sci. Rep.* **10** 9089
microDiamond 2024 *Synthetic Diamond Detector for High-Precision Dosimetry* (available at: www.ptwdosimetry.com/en/products/microdiamond) (Acessed 1 December 2023)
Milluzzo G *et al* 2023 OC-0930 silicon carbide detectors for dosimetry and monitoring of UHDR beams for FLASH radiotherapy *Radiother. Oncol.* **182** S777–S778
Moding E J, Kastan M B and Kirsch D G 2013 Strategies for optimizing the response of cancer and normal tissues to radiation *Nat. Rev. Drug Discov.* **12** 526–42
Montay-Gruel P *et al* 2017 Irradiation in a flash: unique sparing of memory in mice after whole brain irradiation with dose rates above 100Gy/s *Radiother. Oncol.* **124** 365–9
Montay-Gruel P *et al* 2018 X-rays can trigger the FLASH effect: ultra-high dose-rate synchrotron light source prevents normal brain injury after whole brain irradiation in mice *Radiother. Oncol.* **129** 582–8
Montay-Gruel P, Meziani L, Yakkala C and Vozenin M C 2019 Expanding the therapeutic index of radiation therapy by normal tissue protection *Br. J. Radiol.* **92** 20180008
Motta S, Christensen J B, Frei F, Peier P and Yukihara E G 2023 Investigation of TL and OSL detectors in ultra-high dose rate electron beams *Phys. Med. Biol.* **68** 145007
Feasibility study of FLASH radiotherapy for the treatment of symptomatic bone metastases (FAST-01) n.d (available at: https://clinicaltrials.gov/ct2/show/NCT04592887)
Nagy V, Sholom S V, Chumak V V and Desrosiers M F 2002 Uncertainties in alanine dosimetry in the therapeutic dose range *Appl. Radiat. Isot.* **56** 917–29
Nava F, Bertuccio G, Cavallini A and Vittone E 2008 Silicon carbide and its use as a radiation detector material *Meas. Sci. Technol.* **19** 102001
Oesterle R, Gonçalves Jorge P, Grilj V, Bourhis J, Vozenin M C, Germond J F, Bochud F, Bailat C and Moeckli R 2021 Implementation and validation of a beam-current transformer on a medical pulsed electron beam LINAC for FLASH-RT beam monitoring *J. Appl. Clin. Med. Phys.* **22** 165–71
Paz-Martín J, Schüller A, Bourgouin A, González-Castaño D M, Gómez-Fernández N, Pardo-Montero J and Gómez F 2022 Numerical modeling of air-vented parallel plate ionization chambers for ultra-high dose rate applications *Phys. Med.* **103** 147–56
Pedersen K H, Kunugi K A, Hammer C G, Culberson W S and DeWerd L A 2016 Radiation biology irradiator dose verification survey *Radiat. Res.* **185** 163–8
Petersson K, Jaccard M, Germond J F, Buchillier T, Bochud F, Bourhis J, Vozenin M C and Bailat C 2017 High dose-per-pulse electron beam dosimetry—a model to correct for the ion recombination in the advanced Markus ionization chamber *Med. Phys.* **44** 1157–67
Pettersson C and Hettinger G 1967 Dosimetry of high-energy electron radiation based on the ferrous sulphate dosimeter *Acta Radiol. Diagn.* **6** 160–76
Picard S, Burns D T, Roger P, D. Prez L A, Jansen B J and Pooter J A 2017 Key comparison BIPM.RI(I)-K6 of the standards for absorbed dose to water of the VSL, Netherlands and the BIPM in accelerator photon beams *Metrologia* **54** 06005
Picard S, Burns D T, Roger P, Duane S, Bass G A, Manning J W and Shipley D R 2015 Key comparison BIPM.RI(I)-K6 of the standards for absorbed dose to water at 10 g cm^{-2} of the NPL, United Kingdom and the BIPM in accelerator photon beams *Metrologia* **52** 06021
Pimpinella M, Stravato A, Guerra A S, Marinelli M and Verona-Rinati G 2015 81—Monte Carlo calculation of beam quality correction factors for the PTW microDiamond in high energy photon and electron beams *Phys. Med.* **31** e53
Renaud J, Palmans H, Sarfehnia A and Seuntjens J 2020 Absorbed dose calorimetry *Phys. Med. Biol.* **65** 05tr02
Renaud J, Sarfehnia A, Bancheri J and Seuntjens J 2018 Aerrow: a probe-format graphite calorimeter for absolute dosimetry of high-energy photon beams in the clinical environment *Med. Phys.* **45** 414–28
Romano F *et al* 2020 Challenges in dosimetry of particle beams with ultra-high pulse dose rates *J. Phys.: Conf. Ser.* **1662** 012028
Romano F *et al* 2023 First characterization of novel silicon carbide detectors with ultra-high dose rate electron beams for FLASH radiotherapy *Appl. Sci.* **13** 2986
Rossomme S, Lorentini S, Vynckier S, Delor A, Vidal M, Lourenço A and Palmans H 2021 Correction of the measured current of a small-gap plane-parallel ionization chamber in proton beams in the presence of charge multiplication *Z. Med. Phys.* **31** 192–202
Rotblat J, Sutton H C and Dainton F S 1997 The effects of high dose rates of ionizing radiations on solutions of iron and cerium salts *Proc. R. Soc. A* **255** 490–508

Schönfeld A B, Poppinga D, Kranzer R, De Wilde R L, Willborn K, Poppe B and Looe H K 2019 Technical note: characterization of the new microSilicon diode detector *Med. Phys.* **46** 4257–62
Schüler E, Acharya M, Montay-Gruel P, Loo,Jr B W, Vozenin M C and Maxim P G 2022 Ultra-high dose rate electron beams and the FLASH effect: from preclinical evidence to a new radiotherapy paradigm *Med. Phys.* **49** 2082–95
Schuler R H and Allen A O 1957 Radiation chemistry studies with cyclotron beams of variable energy: yields in aerated ferrous sulfate solution1 *J. Am. Chem. Soc.* **79** 1565–72
Schüller A *et al* 2020 The European Joint Research Project UHDpulse—metrology for advanced radiotherapy using particle beams with ultra-high pulse dose rates *Phys. Med.* **80** 134–50
Schüller A, Illemann J, Renner F, Makowski C and Kapsch R P 2017 Traceable charge measurement of the pulses of a 27 MeV electron beam from a linear accelerator *J. Instrum.* **12** 03003
Schüller A, Pojtinger S, Meier M, Makowski C and Kapsch R-P 2019 The Metrological Electron Accelerator Facility (MELAF) for research in dosimetry for radiotherapy *World Congress on Medical Physics and Biomedical Engineering 2018*
Schütte W and Unser K B 1992 Beam current and beam lifetime measurements at the HERA proton storage ring *AIP Conf. Proc.* **281** 225–33
Sehested K, Bjergbakke E, Holm N W and Fricke H 1973 *The Reaction Mechanism of the Ferrous Sulphate Dosimeter at High Dose Rates* (International Atomic Energy Agency (IAEA))
Sellin P J and Vaitkus J 2006 New materials for radiation hard semiconductor detectors *Nucl. Instrum. Methods Phys. Res.* A **557** 479–89
Sharpe P H G and Sephton J P 1988 Alanine dosimetry at NPL—the development of a mailed reference dosimetry service at radiotherapy dose levels *IAEA-SM-356/R6 Proc. Int. symp. on techniques for high dose dosimetry in Industry, Agriculture and Medicine*
Sharpe P H, Rajendran K and Sephton J P 1996 Progress towards an alanine/ESR therapy level reference dosimetry service at NPL *Appl. Radiat. Isot.* **47** 1171–5
Singers Sørensen B, Krzysztof Sitarz M, Ankjærgaard C, Johansen J, Andersen C E, Kanouta E, Overgaard C, Grau C and Poulsen P 2022 In vivo validation and tissue sparing factor for acute damage of pencil beam scanning proton FLASH *Radiother. Oncol.* **167** 109–15
Soliman Y S, Pellicioli P, Beshir W B, Abdel-Fattah A A, Fahim R A, Krisch M and Bräuer-Krisch E 2020 A comparative dosimetry study of an alanine dosimeter with a PTW PinPoint chamber at ultra-high dose rates of synchrotron radiation *Phys. Med.* **71** 161–7
Stephan F *et al* 2022 FLASHlab@PITZ: new R&D platform with unique capabilities for electron FLASH and VHEE radiation therapy and radiation biology under preparation at PITZ *Phys. Med.* **104** 174–87
Subiel A and Romano F 2023 Recent developments in absolute dosimetry for FLASH radiotherapy *Brit. J. Radiol.* **96** 20220560
Sutton H C and Rotblat J 1957 Dose-rate effects in radiation-induced chemical reactions *Nature* **180** 1332–3
Svensson H and Brahme A 1979 Ferrous sulphate dosimetry for electrons: a re-evaluation *Acta Radiol.: Oncol. Radiat. Phys. Biol.* **18** 326–36
Task Group No. 359 FLASH (ultra-high dose rate) radiation dosimetry (TG359) (available at: www.aapm.org/org/structure/default.asp?committee_code=TG359)
Tessonnier T, Verona-Rinati G, Rank L, Kranzer R, Mairani A and Marinelli M 2023 Diamond detectors for dose and instantaneous dose-rate measurements for ultra-high dose-rate scanned helium ion beams *Med. Phys.* **51** 1450–459
The BIPM key comparison database 2023 (www.bipm.org/kcdb/comparison/statistics/key) (accessed 1 September 2023)
Thomas J K and Hart E J 1962 The radiolysis of aqueous solutions at high intensities *Radiat. Res.* **17** 408–18
Torp B, Abrahamsen P, Eriksen S, Høeg P L, Nielsen B R and Bergoz J 1994 Non-intercepting continuous beam current measurement for a high-current ion implanter *Surf. Coat. Technol.* **66** 361–3
Town C D 1967 Effect of high dose rates on survival of mammalian cells *Nature* **215** 847–8
TRS-398 2006 *Absorbed Dose Determination in External Beam Radiotherapy* (International Atomic Energy Agency)
UHDpulse n.d. (http://uhdpulse-empir.eu/) (Accessed 3 May 2023)
Unser K B 1985 Toroidal ac and dc current transformers for beam intensity measurements *Atomkernenerg. Kerntech.* **47** 48–52
Unser K B 1992 The parametric current transformer: a beam current monitor developed for LEP *AIP Conf. Proc.* **252** 266–75
Unser K 1981 A toroidal DC beam current transformer with high-resolution *IEEE Trans. Nucl. Sci.* **23** 2344–6
Verona Rinati G *et al* 2022 Application of a novel diamond detector for commissioning of FLASH radiotherapy electron beams *Med. Phys.* **49** 5513–22
Vörös S, Anton M and Boillat B 2012 Relative response of alanine dosemeters for high-energy electrons determined using a Fricke primary standard *Phys. Med. Biol.* **57** 1413
Vörös S and Stucki G 2007 Simulation Monte Carlo pour la réalisation d'un étalon primaire de la dose absorbée dans l'eau pour des faisceaux d'électrons *Radioprotection* **42** 565–75
Vozenin M-C *et al* 2019 The advantage of FLASH radiotherapy confirmed in mini-pig and cat-cancer patients *Clin. Cancer Res.* **25** 35–42
Williams A J, Burns D T and McEwen M R 1993 *Measurement of the specific heat capacity of the electron-beam grahite calorimeter* NPL Report. RSA(EXT) 40 NPL
Zackrisson B U, Nyström U H and Ostbergh P 1991 Biological response *in vitro* to pulsed high dose rate electrons from a clinical accelerator *Acta oncol.* **30** 747–51